

Removing the influence of centrality fluctuations in the analysis of forward-backward multiplicity correlations in heavy-ion collisions

Ronghua He,^{1,*} Jing Qian,^{1,2} and Lei Huo¹¹*Department of Physics, Harbin Institute of Technology, Harbin 150001, People's Republic of China*²*Department of Physics, The Ohio State University, Columbus, Ohio 43210-1117, USA*

(Received 16 June 2016; published 12 September 2016)

In high-energy heavy-ion collisions, forward-backward multiplicity (FB) correlation strengths are affected greatly by centrality fluctuation and centrality window width. A method called $\text{FB}_{\text{relative}}$ is raised to reduce or remove the influence. This method is tested by a Monte Carlo simulation and is compared with the $\text{FB}_{\text{average}}$ and $\text{FB}_{\text{profile}}$ methods. The $\text{FB}_{\text{relative}}$ method is also used for the HIJING event generator of Au+Au collisions, and comparisons between the correlation strengths of different collision energies $\sqrt{s_{NN}}$ from 7.7 to 200 GeV are shown. As a result, the correlation strengths are all very weak, and the similarities of correlation strengths b of different centrality windows within 0%–50% are obvious, and it is observed that the correlation strengths decrease with the increasing pseudorapidity gap at $|\eta| < 2$.

DOI: [10.1103/PhysRevC.94.034902](https://doi.org/10.1103/PhysRevC.94.034902)

I. INTRODUCTION

The forward-backward multiplicity (FB) correlation is considered to be one of the most important probes of early stages of high-energy heavy-ion collisions [1]. The studies of hadron-hadron collisions show strong FB correlations at $|\eta| < 1$, and the correlation strengths increase with collision energy obviously [2–16]. This phenomenon was explained by using a negative binomial distribution [17–20] and was also studied by models [17,21–36] such as the color glass condensate (CGC) model and the dual parton model (DPM) [37–42]. The CGC model also suggests that the correlations from early stage can spread across a wide range of rapidity [1,33–36,41,43,44].

In recent years, FB correlation strengths were observed at intermediate pseudorapidity of nucleus-nucleus collisions such as Au+Au collisions at $\sqrt{s_{NN}} = 200$ GeV [13,14]. In the experiment of Au+Au collisions at 200 GeV, the FB correlation strengths b were measured as a function of centrality ε and pseudorapidity gap $\Delta\eta$. It was observed that b vs $\Delta\eta$ is flat for the centrality bins 0%–10%, 10%–20%, 20%–30%, and 30%–40% [13,14]. For 50%–60%, b falls exponentially in pseudorapidity, and this phenomenon is similar to the results of the $p\bar{p}$ collisions [5]. It was considered to be the results of short-range correlations [37]. The existence of long-range correlations was predicted in a multiple scattering model of hadron-nucleus interactions [42]. For Au+Au collisions at 200 GeV, the flat correlation strengths b as a function of $\Delta\eta$ were considered to be the sum of the short- and long-range correlations in the framework of the dual parton model of nucleus-nucleus collisions. The short-range parts were calculated by utilizing the b of the pp collisions at $\sqrt{s} = 200$ GeV, which were considered to only include short-range correlations, and the rest of the parts were considered to be the results of long-range correlations [13,37]. The b at $\Delta\eta < 2$ were also compared with the results of a parton string

model [22,23,38] and the similarity is obvious. For 0%–10%, the b of the HIJING model [45] were similar to the results of short-range correlations: b decreases with the increasing $\Delta\eta$. In the CGC model, the long-range correlations were expressed as

$$\sigma_{\text{FB}} = \frac{1}{1 + c\alpha_s^2}, \quad (1)$$

where c increases with $\Delta\eta$ and is related to soft correlated emission, and α_s^2 is related to the centrality [33–36].

On the other hand, FB correlation strengths b were calculated by the $\text{FB}_{\text{average}}$ and $\text{FB}_{\text{profile}}$ methods, and these two methods were described in detail in Ref. [46]. FB correlation strength is defined as Pearson's correlation coefficient of forward multiplicity N_f and backward multiplicity N_b , where N_f and N_b are the numbers of charged particles falling into the forward and backward pseudorapidity intervals $\delta\eta$, respectively,

$$b = \frac{\langle N_b N_f \rangle - \langle N_b \rangle \langle N_f \rangle}{\sqrt{\langle N_b^2 \rangle - \langle N_b \rangle^2} \sqrt{\langle N_f^2 \rangle - \langle N_f \rangle^2}} = \frac{D_{\text{bf}}^2}{D_{\text{bb}} D_{\text{ff}}}, \quad (2)$$

where D_{bf} , D_{bb} , and D_{ff} are the backward-forward, backward-backward, and forward-forward dispersions, respectively. Because these two intervals separate symmetrically around $\eta = 0$ and nucleus-nucleus collisions are symmetrical, Eq. (2) can be also expressed as a linear factor of the relationship between average backward multiplicity and forward multiplicity $\langle N_b(N_f) \rangle = a + bN_f$ [4,42], which can be expressed as

$$b = \frac{\langle N_b N_f \rangle - \langle N_b \rangle \langle N_f \rangle}{\langle N_f^2 \rangle - \langle N_f \rangle^2} = \frac{D_{\text{bf}}^2}{D_{\text{ff}}^2}. \quad (3)$$

For reducing the bias of the results, the centralities were determined by the reference multiplicities N_{ref} , which is the number of charged particles within the η windows other than the used forward and backward intervals [46].

In the $\text{FB}_{\text{average}}$ method, the fluctuations within a centrality window are not taken into account. The results of the $\text{FB}_{\text{average}}$ method were explained by the event mixing of a purely

*ronghuahe2007@163.com

statistical analysis under the assumption that the charged particle multiplicity obeys a negative binomial distribution [17–20]. In this method, the FB correlation is influenced greatly by the centrality window width, and the comparisons of correlation strengths between different centrality windows are obscure [18,19,46–48]. In the $\text{FB}_{\text{profile}}$ method, the obscure b of different centrality windows are still existent (shown in Sec. III in detail), and the b are also influenced by centrality fluctuation equivalent to the fluctuation of reference multiplicity N_{ref} (described in detail in Appendix A). For the reasons above, it is a natural choice to raise a method in which b of a centrality window can be calculated without the influence of centrality fluctuation.

In Sec. II, the $\text{FB}_{\text{average}}$ and $\text{FB}_{\text{profile}}$ methods are described summarily, and then we describe a new method called $\text{FB}_{\text{relative}}$. In Sec. III, to test the $\text{FB}_{\text{relative}}$ method, a Monte Carlo (MC) simulation with an adjustable correlation is built, and these three methods are compared for different centrality windows. For the $\text{FB}_{\text{relative}}$ method, the FB correlation strengths b of HIJING of Au+Au collisions from 7.7 to 200 GeV are also shown. A summary is given in Sec. IV.

II. METHODS

In this paper, the widths of the forward and backward intervals are both set to $\delta\eta = 0.2$. The pseudorapidity gaps are set to $\Delta\eta = 0.2, 0.4, 0.6, 0.8, 1.0, 1.2, 1.4, 1.6,$ and 1.8 . Centralities are decided by the reference multiplicities N_{ref} , and every η gap corresponds to some particular reference window. For $\Delta\eta = 0.2, 0.4,$ and 0.6 , the reference windows are set to $0.5 < |\eta| < 1.0$. For $\Delta\eta = 0.8$ and 1.0 , N_{ref} is the sum of the multiplicities in $|\eta| < 0.3$ and $0.8 < |\eta| < 1.0$. For $\Delta\eta = 1.2, 1.4, 1.6, 1.8,$ and bigger pseudorapidity gaps, the reference windows are set to $|\eta| < 0.5$. It is worth noting that the sums of the reference window widths $\Delta\eta_{\text{ref}}$ are all equal to 1.0 for different pseudorapidity gaps $\Delta\eta$. These parameters above are set the same as in Ref. [46] and are all illustrated in Fig. 1.

In the $\text{FB}_{\text{average}}$ method, $\langle N_f \rangle, \langle N_b \rangle, \langle N_b N_f \rangle,$ and $\langle N_f^2 \rangle$ are the averages over the events in centrality windows. D_{bf} and D_{ff} are calculated by utilizing these averages [46]. The measured

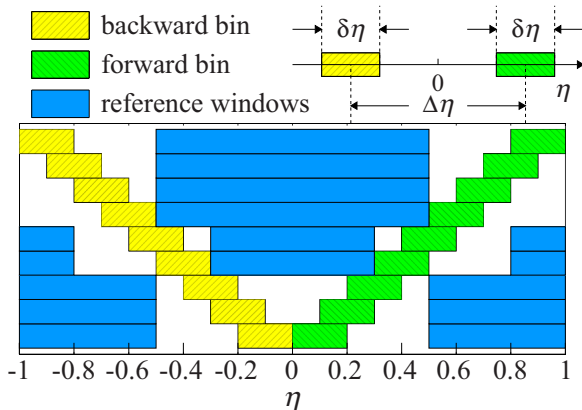


FIG. 1. Sets of forward and backward η windows for different separation $\Delta\eta$.

correlation strengths b are dominated by the mixing of different centrality events [17–20].

In the $\text{FB}_{\text{profile}}$ method, $\langle N_f \rangle, \langle N_b \rangle, \langle N_b N_f \rangle,$ and $\langle N_f^2 \rangle$ are fitted as functions of N_{ref} . Linear fits are made for $\langle N_f \rangle$ and $\langle N_b \rangle$, and second-order polynomial fits are made for $\langle N_b N_f \rangle$ and $\langle N_f^2 \rangle$. D_{bf} and D_{ff} are calculated by using the fitting parameters, and are normalized by all the events in the centrality window [46]. It is worth noting that the FB correlation strengths b calculated by using the $\text{FB}_{\text{profile}}$ method are very sensitive to the size of the reference-multiplicity range and the fitting range. This phenomenon is shown in detail in Appendix A.

In the following parts of this section, we will describe a new method called the $\text{FB}_{\text{relative}}$ method. In this method, the forward and backward multiplicities N_f and N_b are taken place by relative multiplicities n_f and n_b (defined in detail later), respectively, to remove the fluctuation of centrality, and the biases caused by the fluctuation of N_{ref} are also modified.

The centralities are vague because of the biases caused by N_{ref} . For a certain centrality ε (not a centrality window), b can be expressed as

$$b = \frac{\langle N_b N_f \rangle_\varepsilon - \langle N_b \rangle_\varepsilon \langle N_f \rangle_\varepsilon}{\langle N_f^2 \rangle_\varepsilon - \langle N_f \rangle_\varepsilon^2}, \quad (4)$$

where $\langle \dots \rangle_\varepsilon$ stands for the average over the events with centrality ε . For a certain centrality ε , the expectation of the reference multiplicities N_{ref} is written as μ_ε in the following derivation, and it also can be expressed as a function of centrality, which is written as $\mu(\varepsilon)$. Therefore, b of a certain centrality ε can be expressed as

$$b = \frac{\langle \frac{N_b N_f}{\mu_\varepsilon^2} \rangle_\varepsilon - \langle \frac{N_b}{\mu_\varepsilon} \rangle_\varepsilon \langle \frac{N_f}{\mu_\varepsilon} \rangle_\varepsilon}{\langle \frac{N_f^2}{\mu_\varepsilon^2} \rangle_\varepsilon - \langle \frac{N_f}{\mu_\varepsilon} \rangle_\varepsilon^2} = \frac{\langle n_b^* n_f^* \rangle_\varepsilon - \langle n_b^* \rangle_\varepsilon \langle n_f^* \rangle_\varepsilon}{\langle n_f^{*2} \rangle_\varepsilon - \langle n_f^* \rangle_\varepsilon^2}, \quad (5)$$

where $n_f^* = N_f/\mu_\varepsilon$ and $n_b^* = N_b/\mu_\varepsilon$. Equation (5) can be also expressed as an equivalent equation

$$(\langle n_f^{*2} \rangle_\varepsilon - \langle n_f^* \rangle_\varepsilon^2) b = \langle n_f^* n_b^* \rangle_\varepsilon - \langle n_f^* \rangle_\varepsilon \langle n_b^* \rangle_\varepsilon. \quad (6)$$

In the centrality window, we assume that the FB correlation strengths b of different centralities in the window are equal to each other, and the probability density function of ε is denoted by $f(\varepsilon)$. Therefore, by integrating both sides of Eq. (6), b can be expressed as

$$\begin{aligned} b &= \frac{\int (\langle n_f^* n_b^* \rangle_\varepsilon - \langle n_f^* \rangle_\varepsilon \langle n_b^* \rangle_\varepsilon) f(\varepsilon) d\varepsilon}{\int (\langle n_f^{*2} \rangle_\varepsilon - \langle n_f^* \rangle_\varepsilon^2) f(\varepsilon) d\varepsilon} \\ &= \frac{\langle n_f^* n_b^* \rangle - \int \langle n_f^* \rangle_\varepsilon \langle n_b^* \rangle_\varepsilon f(\varepsilon) d\varepsilon}{\langle n_f^{*2} \rangle - \int \langle n_f^* \rangle_\varepsilon^2 f(\varepsilon) d\varepsilon}, \end{aligned} \quad (7)$$

where $\langle \dots \rangle$ without a subscript stands for the average over a centrality window, and the equations $\int \langle n_f^* n_b^* \rangle_\varepsilon f(\varepsilon) d\varepsilon = \langle n_f^* n_b^* \rangle$ and $\int \langle n_f^{*2} \rangle_\varepsilon f(\varepsilon) d\varepsilon = \langle n_f^{*2} \rangle$ are utilized in Eq. (7). For charged particle multiplicities N_{ch} , the shapes of distributions $\frac{dN_{\text{ch}}}{N_{\text{ch}} d\eta}$ of different centralities ε are nearly the same in a narrow centrality window: the narrower the centrality window, the more similar the shapes. So the averages $\langle n_f^* \rangle_\varepsilon$ for different centralities ε are all approximate to the average $\langle n_f^* \rangle$ over the

centrality window. Therefore, b can be simplified to

$$b = \frac{\langle n_f^* n_b^* \rangle - \langle n_f^* \rangle \langle n_b^* \rangle}{\langle n_f^{*2} \rangle - \langle n_f^* \rangle^2}. \quad (8)$$

It is worth noting that Eq. (8) is not used to calculate the FB correlation strength b , because the expectation μ_ε of reference multiplicities N_{ref} for a certain centrality ε cannot be measured directly.

On the other hand, for a measured N_{ref} , we assume that the probability of corresponding μ_ε obeys a Gaussian distribution

$$g(\mu_\varepsilon; N_{\text{ref}}, \sqrt{N_{\text{ref}}}) = \frac{1}{\sqrt{2\pi N_{\text{ref}}}} e^{-\frac{(\mu_\varepsilon - N_{\text{ref}})^2}{2N_{\text{ref}}}}, \quad (9)$$

where $\sqrt{N_{\text{ref}}}$ and μ_ε can be thought to be the statistical error and truth value of N_{ref} , respectively. This requires a few caveats. The Gaussian approximation is not suited very well for the most central collisions (such as the centrality windows covering 0%-5%). The drawbacks are explained in Appendix B, and the effects are shown in Sec. III. Anyhow, if the approximation is used, for a centrality window,

$$\begin{aligned} \left\langle \frac{\mu_\varepsilon}{N_{\text{ref}}} \right\rangle &= \iint \frac{\mu_\varepsilon}{N_{\text{ref}}} g(\mu_\varepsilon; N_{\text{ref}}, \sqrt{N_{\text{ref}}}) h(N_{\text{ref}}) dN_{\text{ref}} = 1, \\ \left\langle \frac{\mu_\varepsilon^2}{N_{\text{ref}}^2} \right\rangle &= \iint \frac{\mu_\varepsilon^2}{N_{\text{ref}}^2} g(\mu_\varepsilon; N_{\text{ref}}, \sqrt{N_{\text{ref}}}) h(N_{\text{ref}}) dN_{\text{ref}} \\ &= \int \left(1 + \frac{1}{N_{\text{ref}}} \right) h(N_{\text{ref}}) dN_{\text{ref}} = 1 + \left\langle \frac{1}{N_{\text{ref}}} \right\rangle, \end{aligned} \quad (10)$$

where $h(N_{\text{ref}})$ is the distribution function of N_{ref} in the centrality window. We define the forward and backward relative multiplicities as $n_f \equiv N_f/N_{\text{ref}}$ and $n_b \equiv N_b/N_{\text{ref}}$, respectively. By utilizing Eq. (10), the relationships between the averages $\langle n_f \rangle$, $\langle n_b \rangle$, $\langle n_f n_b \rangle$, $\langle n_f^2 \rangle$ and $\langle n_f^* \rangle$, $\langle n_b^* \rangle$, $\langle n_f^* n_b^* \rangle$, $\langle n_f^{*2} \rangle$ over a centrality window can be expressed as

$$\begin{aligned} \langle n_f \rangle &= \left\langle \frac{N_f}{N_{\text{ref}}} \frac{\mu_\varepsilon}{N_{\text{ref}}} \right\rangle = \left\langle \frac{N_f}{N_{\text{ref}}} \right\rangle \left\langle \frac{\mu_\varepsilon}{N_{\text{ref}}} \right\rangle = \langle n_f^* \rangle, \\ \langle n_b \rangle &= \left\langle \frac{N_b}{N_{\text{ref}}} \frac{\mu_\varepsilon}{N_{\text{ref}}} \right\rangle = \left\langle \frac{N_b}{N_{\text{ref}}} \right\rangle \left\langle \frac{\mu_\varepsilon}{N_{\text{ref}}} \right\rangle = \langle n_b^* \rangle, \\ \langle n_f^2 \rangle &= \left\langle \frac{N_f^2}{N_{\text{ref}}^2} \frac{\mu_\varepsilon^2}{N_{\text{ref}}^2} \right\rangle = \langle n_f^{*2} \rangle \left(1 + \left\langle \frac{1}{N_{\text{ref}}} \right\rangle \right), \\ \langle n_f n_b \rangle &= \left\langle \frac{N_f N_b}{N_{\text{ref}}^2} \frac{\mu_\varepsilon^2}{N_{\text{ref}}^2} \right\rangle = \langle n_f^* n_b^* \rangle \left(1 + \left\langle \frac{1}{N_{\text{ref}}} \right\rangle \right), \end{aligned} \quad (11)$$

where the correlations between N_f (or N_b) and N_{ref} are ignored. By taking Eq. (11) into Eq. (8), b can be expressed as

$$b = \frac{\langle n_f n_b \rangle - \left(1 + \left\langle \frac{1}{N_{\text{ref}}} \right\rangle \right) \langle n_f \rangle \langle n_b \rangle}{\langle n_f^2 \rangle - \left(1 + \left\langle \frac{1}{N_{\text{ref}}} \right\rangle \right) \langle n_f \rangle^2}. \quad (12)$$

The variables n_f , n_b , and N_{ref} in Eq. (12) can be all determined experimentally, and this expression dodges the direct and accurate measurements of centralities. By introducing the relative multiplicities, the differences between events with different centralities within a centrality window are removed. In other words, the correlations caused by the mixing of events with different centralities can be eliminated. The effect of the

FB_{relative} method is tested by a Monte Carlo model in the next section.

On the other hand, if we ignore the biases of N_{ref} , false FB correlation strengths can be calculated by a similar formula including the forward and backward relative multiplicities n_f and n_b . It is shown in detail in Appendix C.

III. MONTE CARLO TESTING AND RESULTS OF HIJING

To test the FB_{relative} method, a Monte Carlo (MC) simulation with a controllable FB correlation is made. The charged particle multiplicity distribution $d\sigma/dN_{\text{ch}}$ at $|\eta| < 1$ is set to that of Au+Au collisions of the HIJING event generator at $\sqrt{s_{NN}} = 200$ GeV, where σ and N_{ch} stand for the total cross section of the A-A collision and the charged particle multiplicity, respectively. The pseudorapidity distribution $dN_{\text{ch}}/d\eta$ is set to be flat at $|\eta| < 1$. For a Monte Carlo event, the particles are divided into two parts: the correlated part (CP) and the uncorrelated part (UCP), and the proportion of the correlated part is denoted as α . For an event with N_{ch} particles at $|\eta| < 1$, the αN_{ch} particles belong to CP. These particles of CP can be divided into $\alpha N_{\text{ch}}/2$ pairs, and the pseudorapidities of a pair of particles are set to η and $-\eta$, where η is a random number between 0 and 1. For the remaining part of the event, the pseudorapidities of $(1 - \alpha)N_{\text{ch}}$ UCP particles are set to random numbers between -1 and 1 independently. For such a MC source, b can be expressed as

$$b = \frac{\alpha - \alpha p - p}{1 - \alpha p - p}, \quad (13)$$

where p is the probability of a particle falling into the forward (or backward) bin, and in this paper, p is equal to $\delta\eta/(\eta_{\text{max}} - \eta_{\text{min}}) = 0.1$, where $(\eta_{\text{min}}, \eta_{\text{max}})$ is the range of pseudorapidity in the MC model. Equation (13) is deduced in detail in Appendix D.

When α of the MC source is set to 0, the correlation strengths b are calculated as a function of the centrality and pseudorapidity gap $\Delta\eta$, and the results of the FB_{average}, FB_{profile}, and FB_{relative} methods are shown in Figs. 2(a), 2(b), and 2(c), respectively. There are no additional correlations in the MC source, but positive correlations as the results of the

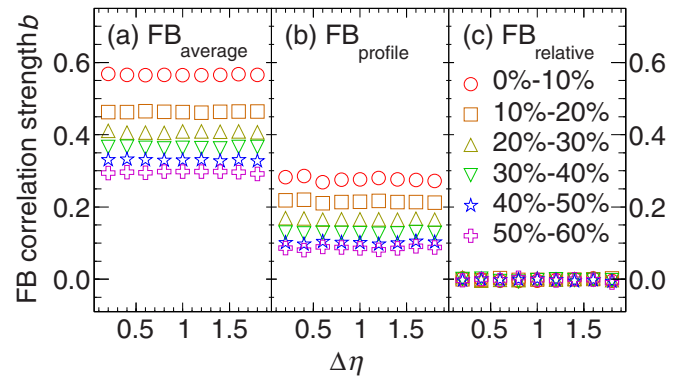


FIG. 2. FB correlation strengths b of different centrality windows of the MC source without additional FB correlations ($\alpha = 0$) for the FB_{average}, FB_{profile}, and FB_{relative} methods.

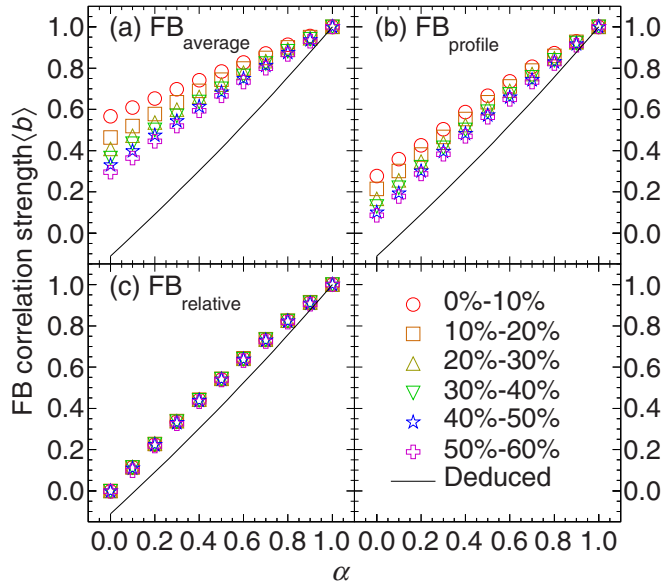


FIG. 3. Averages of b over $\Delta\eta$ from 0 to 2 for the $\text{FB}_{\text{average}}$, $\text{FB}_{\text{profile}}$, and $\text{FB}_{\text{relative}}$ methods. $\langle b \rangle$ is plotted as a function of correlation parameter α . The results of Eq. (13) are denoted by “Deduced.”

$\text{FB}_{\text{average}}$ and $\text{FB}_{\text{profile}}$ methods are obvious. The results of the $\text{FB}_{\text{relative}}$ method are more reasonable: the correlation strengths b are close to zero and there are nearly no differences between b of different centrality windows.

For different α from 0 to 1, the FB correlation strengths b are calculated by these three methods, and the comparisons of b of these three methods are shown in Fig. 3. The widths of the forward and backward bins $\delta\eta$ are always equal to 0.2 and symmetrical around $\eta = 0$, so there are no differences between b of different pseudorapidity gaps $\Delta\eta$ for such a MC source. Therefore, for a certain α , the averages of b of different $\Delta\eta$ are made and shown in Fig. 3. For a certain α , b should be a constant as Eq. (13) for this MC source, and b of different centrality windows should be the same. For the $\text{FB}_{\text{average}}$ and $\text{FB}_{\text{profile}}$ methods, the correlation strengths b of centrality windows are different from each other obviously for the same α . For the $\text{FB}_{\text{relative}}$ method, there are nearly no differences between b of different centrality windows. For the $\text{FB}_{\text{relative}}$ method, the differences between b and Eq. (13) are thought to be the result of ignoring the correlations between N_f (or N_b) and N_{ref} and the correlations between the particles in reference windows.

For the $\text{FB}_{\text{relative}}$ method, the correlation strengths b of Au+Au collisions of the HIJING event generator at $\sqrt{s_{NN}} = 7.7\text{--}200$ GeV are shown in Fig. 4. The b for 0%–10%, 10%–20%, 20%–30%, and 40%–50% are shown. It is common for these collision energies that b of different centrality windows are similar to each other obviously. The weak FB correlations can be seen at $\Delta\eta < 2$, and the correlation strengths b decrease with the increasing pseudorapidity $\Delta\eta$. Weak negative correlations are also seen at long range such as $1 < \Delta\eta < 2$. If the particles emit randomly and independently without any additional correlations, a negative b is a natural

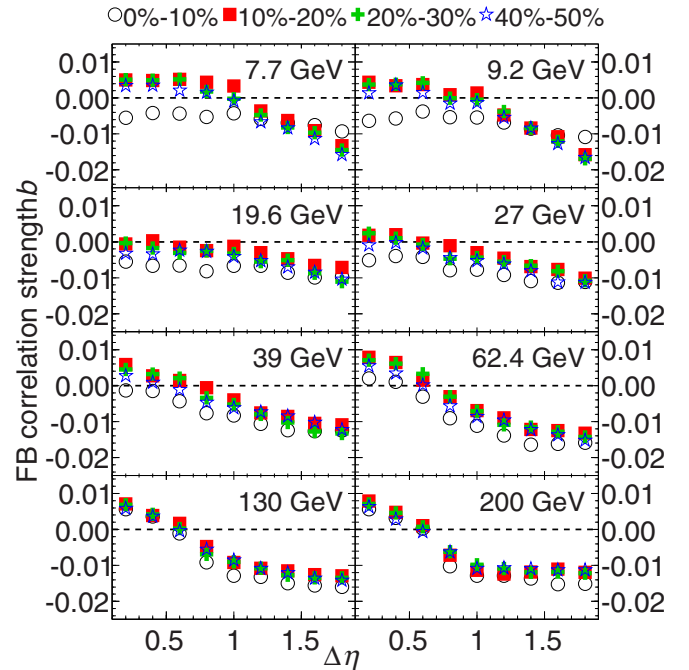


FIG. 4. FB correlation strengths b of different centrality windows of HIJING event generator of Au+Au collisions at $\sqrt{s_{NN}} = 7.7$ to 200 GeV for the $\text{FB}_{\text{relative}}$ method.

result caused by a binomial distribution. But the weak negative correlations can be overwhelmed easily by the centrality fluctuation. It is notable that the correlation strengths b of 0%–10% are different from other centrality windows especially for the lower collision energies. We consider that this phenomenon is caused by the unsuitable Gaussian approximation alluded to in Sec. II and explained in detail in Appendix B.

On the other hand, to see the tendency of b vs $\sqrt{s_{NN}}$, the b for centrality windows within 0%–50% of different $\Delta\eta$ as a function of $\sqrt{s_{NN}}$ are shown in Fig. 5. In Fig. 5, the negative correlation strengths are seen obviously at long range, such as $\Delta\eta = 1.8$. Additionally, the centrality window 0%–5% is avoided in Fig. 5. In general, the differences between b of different collision energies are more obvious than these of different centrality windows. In other words, b is more sensitive to collision energy than to centrality. For this phenomenon, we give a rough explanation. We guess that the FB correlations of nuclear-nuclear collisions is dominated by the particles emitting from the same sources. A fireball of a nuclear-nuclear collision is made up by sources of the nucleon-nucleon collisions. The number of sources in a collision is affected greatly by centrality, but the property of a source is dominated by collision energy. The FB correlations without centrality fluctuations should not be influenced greatly by superposition of similar sources in an event. Therefore, FB correlations will not be obviously influenced by centrality.

The decreasing $b(\Delta\eta)$ were also seen in the pp collisions [3–13], though the b of the pp collisions were higher and can be understood as a combined result of centrality fluctuations and short-range correlations. In the pp collisions, FB correlation strengths b were calculated by using the $\text{FB}_{\text{average}}$

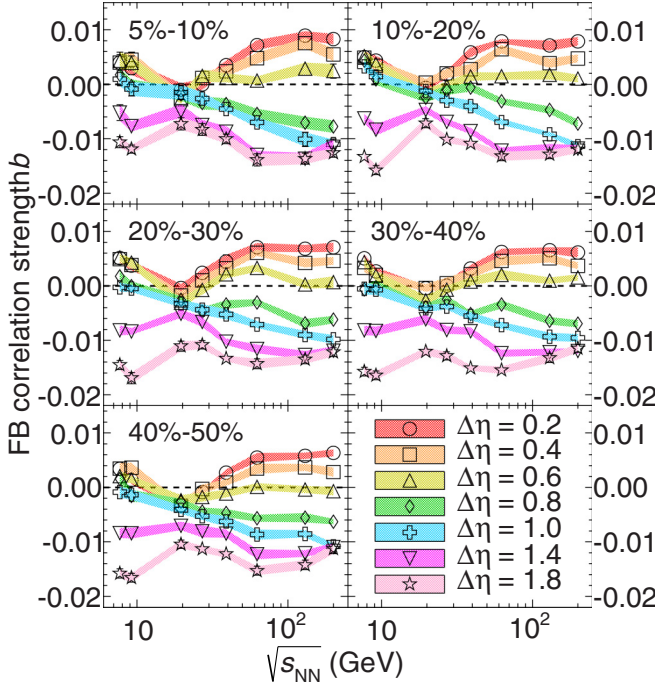


FIG. 5. FB correlation strengths b of different pseudorapidity gaps $\Delta\eta$ as a function of collision energy $\sqrt{s_{NN}}$ from 7.7 to 200 GeV for the $\text{FB}_{\text{relative}}$ method.

method, and the positive correlation strengths were considered to be dominated by the mixing of events under an assumption of a negative binomial distribution [7,17–19]. In the process of calculating b of pp collisions, the mixing of events is equivalent to the centrality fluctuation, so that the higher b is a natural result. Therefore, the weak correlation strengths around 0 for the $\text{FB}_{\text{relative}}$ method are compatible with the obviously positive correlations in pp collisions for the $\text{FB}_{\text{average}}$ method which did not take into account the centrality fluctuation.

Weak correlations were also seen in the model studies of two-particle-rapidity correlation functions of nuclear-nuclear collisions. The relationship between the rapidity (or pseudorapidity) bins were expressed as the correlation functions $C(\eta_1, \eta_2) = \frac{\rho_2(\eta_1, \eta_2)}{\rho_1(\eta_1)\rho_1(\eta_2)}$ or some equivalent formulas, where $\rho_1(\eta)$ and $\rho_2(\eta_1, \eta_2)$ are the inclusive and double inclusive distributions, respectively [2,49–55]. In Ref. [49] (Figs. 11 and 13), weak correlations were observed obviously for the AMPT (a multiphase transport) model [21] and the HIJING model [45] of Pb+Pb collisions at $\sqrt{s_{NN}} = 2.76$ TeV with impact parameters equal to 8 fm. Some negative correlations were also seen in Ref. [49] at long range, where $C(\eta_1, \eta_2)$ less than 1 were observed. Both the FB correlation strength b less than 0 and the correlation function C less than 1 reflect negative correlations. In sum, though the correlations measured by the $\text{FB}_{\text{relative}}$ method are very weak and even negative, it is not an anomalous result.

It is worth noting that it is difficult to distinguish fluctuations caused by different reasons, such as nucleon-nucleon collision numbers fluctuation in nuclear-nuclear collisions, string number fluctuations, and statistical fluctuations of reference multiplicities. The observed long-range correlations can be

considered to be influenced by these kinds of fluctuations. In the $\text{FB}_{\text{relative}}$ method, we try to remove the influence of centrality fluctuations, but the effects of these kinds of fluctuations above are also reduced or removed, not only the influence of centrality fluctuations.

IV. SUMMARY

A new method called $\text{FB}_{\text{relative}}$ was used to calculate the forward-backward multiplicity correlation strength b as a function of centrality and pseudorapidity gap $\Delta\eta$. In this method, the forward and backward multiplicities N_f and N_b are replaced by the forward and backward relative multiplicities n_f and n_b , respectively, to remove the influence caused by centrality fluctuations, and the biases caused by reference multiplicities are modified. This method was tested by a Monte Carlo simulation with a controllable correlation factor α , and comparisons between the $\text{FB}_{\text{average}}$, $\text{FB}_{\text{profile}}$, and $\text{FB}_{\text{relative}}$ methods were made. For the $\text{FB}_{\text{relative}}$ method, when the correlation parameter α of the MC model was set to the same value for different centrality windows, the measured correlation strengths b approached the deduced results [Eq. (13)], and this method did not cause additional differences between b of different centrality windows. But in the $\text{FB}_{\text{average}}$ and $\text{FB}_{\text{profile}}$ methods, the additional differences are obvious. With the $\text{FB}_{\text{relative}}$ method, the similarity of b of different centrality windows is observed for Au+Au collisions of the HIJING event generator at $\sqrt{s_{NN}} = 7.7\text{--}200$ GeV. For the HIJING event generator, b falls with increasing pseudorapidity gap at $\Delta\eta < 2$. The weak correlation strengths less than 0.1 and negative b at $1 < \Delta\eta < 2$ are observed. On the other hand, with the $\text{FB}_{\text{relative}}$ method, b is more sensitive to collision energy $\sqrt{s_{NN}}$ than to the centrality for the HIJING data. We hope the $\text{FB}_{\text{relative}}$ method can be tested by using experimental data.

ACKNOWLEDGMENT

We thank Yan Yang for his advice and discussions.

APPENDIX A: SENSITIVITY OF b TO REFERENCE WINDOWS AND FITTING RANGE IN $\text{FB}_{\text{profile}}$ METHOD

In the $\text{FB}_{\text{profile}}$ method, $\langle N_f \rangle$, $\langle N_b \rangle$, $\langle N_f^2 \rangle$, and $\langle N_f N_b \rangle$ are counted in reference multiplicity bins (widths are equal to 1). For a certain reference multiplicity bin, some events of different centralities are counted together. Therefore, if we widen the reference windows on the pseudorapidity η axis, the widths of reference multiplicity bins are still equal to 1 but the mixing of events will be over a narrower centrality range. Though seemingly the reference multiplicity bin width may be narrow enough, the b of the events of Au+Au collisions produced by the HIJING event generator at $\sqrt{s_{NN}} = 200$ GeV shows that the results of the $\text{FB}_{\text{profile}}$ method are sensitive to the sum of the widths of reference windows. The sum of the widths of reference windows is denoted by $\Delta\eta_{\text{ref}}$, and the values of $\Delta\eta_{\text{ref}}$ are set to 0.4, 0.6, 1.0 (used in Ref. [46]), 1.2, and 1.4, respectively, to see the sensitivity of b to $\Delta\eta_{\text{ref}}$. As shown in Fig. 6, the differences of b between different windows are

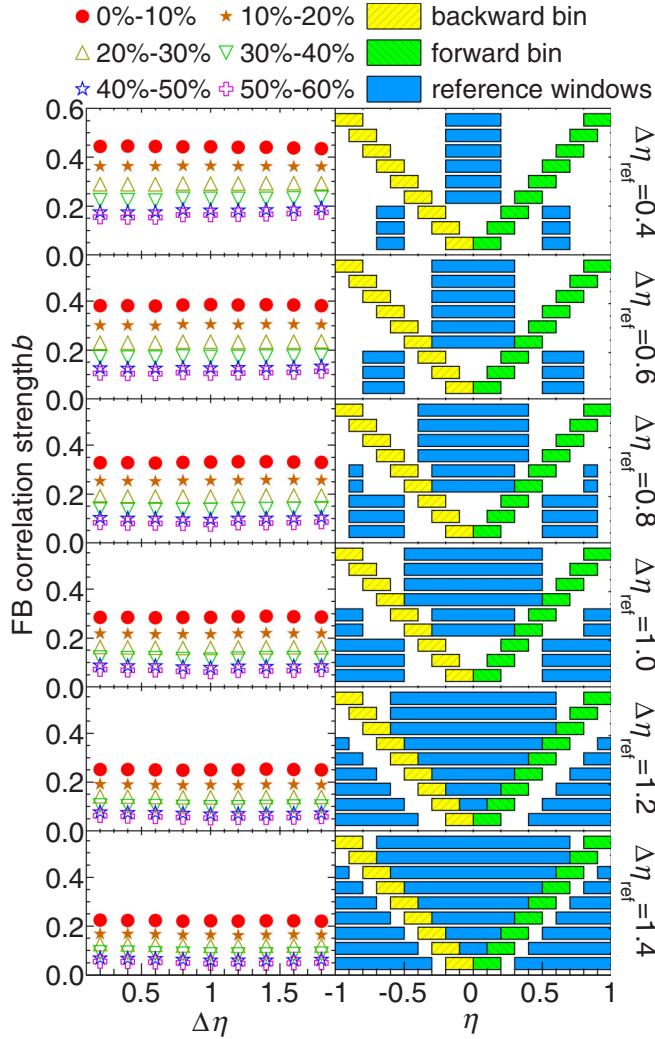


FIG. 6. FB correlation strengths b of different reference windows for HIJING event generator at $\sqrt{s_{NN}} = 200$ GeV by using the $\text{FB}_{\text{profile}}$ method. The sums of reference-window widths are denoted by $\Delta\eta_{\text{ref}}$.

smaller for the bigger $\Delta\eta_{\text{ref}}$. It is worth mentioning that there are no cuts used for the HIJING data.

In the $\text{FB}_{\text{profile}}$ method, $\langle N_f \rangle$, $\langle N_b \rangle$, $\langle N_f^2 \rangle$, and $\langle N_f N_b \rangle$ are plotted as a function of N_{ref} , and linear fits to $\langle N_f \rangle$ and $\langle N_b \rangle$ and second-order polynomial fits to $\langle N_f^2 \rangle$ and $\langle N_f N_b \rangle$ are made [46]. We consider that the fitting over all reference bins is too rough so that the b of a centrality window is influenced by the other centrality windows. To know the effect of the fitting range, we calculate b of different centrality windows with different fitting ranges. As shown in Figs. 7(a)–7(c), the centrality windows and the fitting ranges are marked in the right pads. In the piecewise fitting procedure, b of a certain centrality window is calculated by using the parameters of fitting over the same centrality window. The results of the piecewise fitting are similar with the averages of the correlation strengths of the reference multiplicity bins in the corresponding centrality window, as shown in Fig. 7(d). The comparisons above show that b of the $\text{FB}_{\text{profile}}$ method is sensitive to the fitting range. In addition, we consider that the

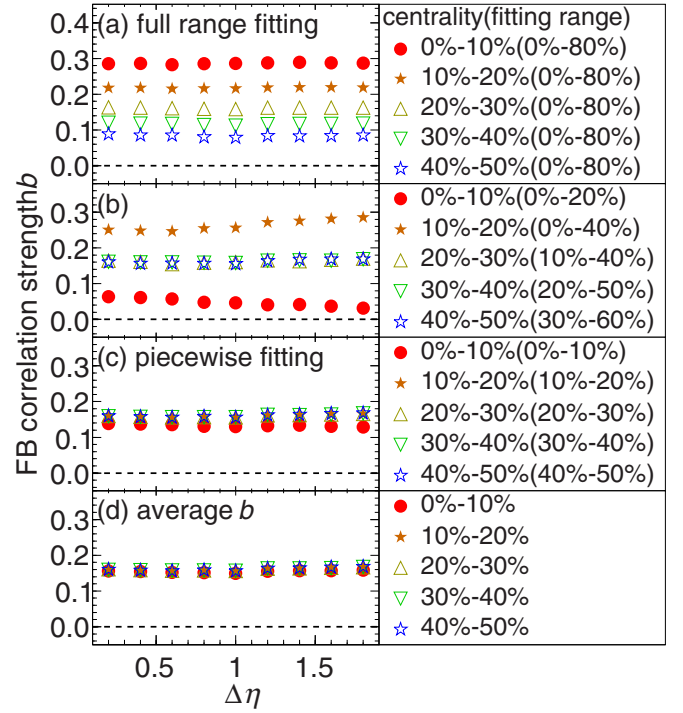


FIG. 7. Sensitivity of the FB correlation strengths b to the fitting range for the $\text{FB}_{\text{profile}}$ method. (a) Full range fitting. (b) Fitting near the centrality windows. (c) Results of piecewise fitting. (d) Averages of b of the reference bins within the centrality windows. The centrality windows and corresponding fitting ranges are shown in the right column.

positive correlations are dominated by the biases of reference multiplicity N_{ref} ; the fluctuation of N_{ref} causes a natural mixing of events of different centralities.

In summary, the results of the $\text{FB}_{\text{profile}}$ method are sensitive to the sum of the widths of reference windows $\Delta\eta_{\text{ref}}$ and the fitting range.

APPENDIX B: DRAWBACKS OF THE GAUSSIAN APPROXIMATION

In Sec. III, a Gaussian approximation is utilized to modify the bias caused by the fluctuation of the reference multiplicity N_{ref} . In this approximation, the truth value of N_{ref} is denoted by μ_ε , and for a certain N_{ref} , the distribution of μ_ε is expressed as a Gaussian function $g(\mu_\varepsilon; N_{\text{ref}}, \sqrt{N_{\text{ref}}}) = \frac{1}{\sqrt{2\pi N_{\text{ref}}}} e^{-\frac{(\mu_\varepsilon - N_{\text{ref}})^2}{2N_{\text{ref}}}}$ [Eq. (9)]. Indeed, the probability distribution of μ_ε and N_{ref} can be expressed more accurately as

$$F(\mu_\varepsilon, N_{\text{ref}}) = H(\mu_\varepsilon) \frac{1}{\sqrt{2\pi \mu_\varepsilon}} e^{-\frac{(N_{\text{ref}} - \mu_\varepsilon)^2}{2\mu_\varepsilon}}, \quad (\text{B1})$$

where $H(\mu_\varepsilon)$ is the distribution of μ_ε . It is reasonable that μ_ε and $\sqrt{\mu_\varepsilon}$ can be understood to be the truth value and statistical error of N_{ref} , respectively. When $H(\mu_\varepsilon)$ is flat and N_{ref} is big enough so that $\sqrt{N_{\text{ref}}}$ is around the value of $\sqrt{\mu_\varepsilon}$, then $F(\mu_\varepsilon, N_{\text{ref}})$ can be expressed approximately as Eq. (9). But for most central events such as 0%–5%, these conditions of the approximation no longer apply; $H(\mu_\varepsilon)$ falls to 0 quickly when

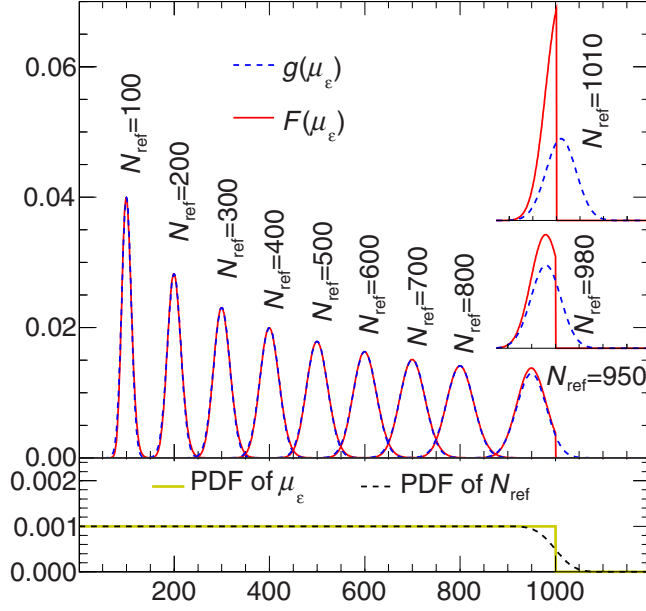


FIG. 8. On the bottom graph, the probability distribution function (PDF) of μ_ϵ is set to an even function $H(\mu_\epsilon)$, and the PDF of N_{ref} is equal to $\int H(\mu_\epsilon) \exp[-\frac{(N_{\text{ref}}-\mu_\epsilon)^2}{2\mu_\epsilon}] d\mu_\epsilon$. On the top graph, for different N_{ref} , PDFs of μ_ϵ are calculated as $g(\mu_\epsilon)$ [Eq. (9)] and $F(\mu_\epsilon)$ [Eq. (B1)].

centrality is close to 0%. Especially for the events with the biggest N_{ref} , μ_ϵ is always less than N_{ref} . Figure 8 illustrates this phenomenon. To explain it accessibly, we assume the probability distribution function (PDF) of μ_ϵ , $H(\mu_\epsilon)$ is even between 0 and 1000. The PDF of N_{ref} can be calculated by integrating $F(\mu_\epsilon, N_{\text{ref}})$ over μ_ϵ . For a certain N_{ref} , $g(\mu_\epsilon)$ and $F(\mu_\epsilon)$ stand for Eq. (9) and Eq. (B1), respectively. From the comparisons between $g(\mu_\epsilon)$ and $F(\mu_\epsilon)$ for different N_{ref} in Fig. 8, it is seen that the differences between $g(\mu_\epsilon)$ and $F(\mu_\epsilon)$ are obvious for high N_{ref} (where the PDF of N_{ref} falls to 0 quickly). In sum, when the $\text{FB}_{\text{relative}}$ method is used, the most central events (0%–5%) should be avoided.

APPENDIX C: SIMPLE $\text{FB}_{\text{relative}}$ METHOD WITHOUT MODIFICATION OF THE N_{ref} FLUCTUATION

If we ignore the biases of N_{ref} , for a certain N_{ref} in a centrality window, FB correlation strengths b can be expressed as

$$b_{N_{\text{ref}}} = \frac{\langle N_f N_b \rangle_{N_{\text{ref}}} - \langle N_f \rangle_{N_{\text{ref}}} \langle N_b \rangle_{N_{\text{ref}}}}{\langle N_f^2 \rangle_{N_{\text{ref}}} - \langle N_f \rangle_{N_{\text{ref}}}^2} = \frac{\langle n_f n_b \rangle_{N_{\text{ref}}} - \langle n_f \rangle_{N_{\text{ref}}} \langle n_b \rangle_{N_{\text{ref}}}}{\langle n_f^2 \rangle_{N_{\text{ref}}} - \langle n_f \rangle_{N_{\text{ref}}}^2}, \quad (\text{C1})$$

where $\langle \dots \rangle_{N_{\text{ref}}}$ stands for the average over the events with the same reference multiplicity N_{ref} , and definitions $n_f \equiv N_f/N_{\text{ref}}$ and $n_b \equiv N_b/N_{\text{ref}}$ (defined in Sec. II) are utilized. Just like the derivation in Sec. II, for a centrality window, the FB correlation strength can be expressed as

$$b = \frac{\langle n_f n_b \rangle - \langle n_f \rangle \langle n_b \rangle}{\langle n_f^2 \rangle - \langle n_f \rangle^2}. \quad (\text{C2})$$

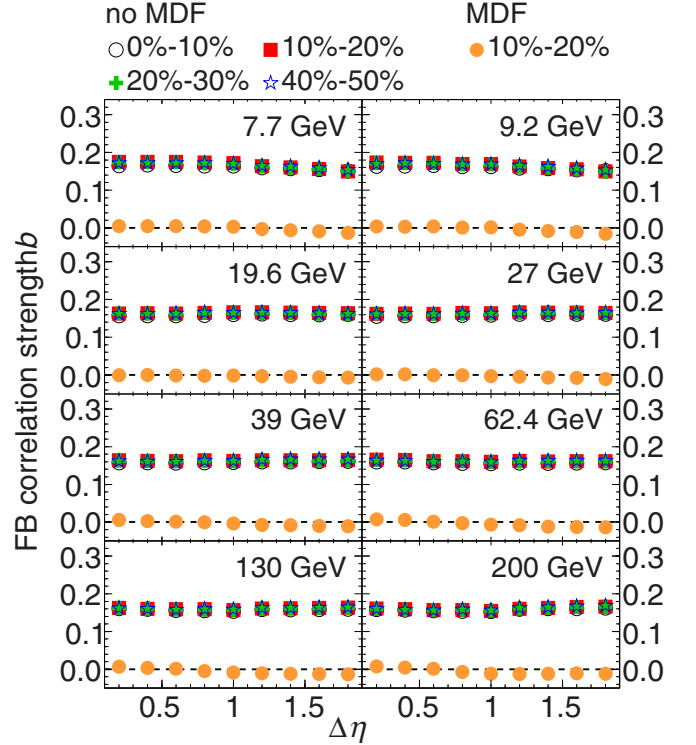


FIG. 9. By using Eq. (C2), the FB correlation strengths b of different centrality windows for Au+Au collisions of the HIJING event generator at $\sqrt{s_{NN}} = 7.7\text{--}200$ GeV are shown, and are denoted by “o MDF” short for “no modification”. The results calculated with Eq. (12) are denoted by “MDF”.

The b of HIJING events at $\sqrt{s_{NN}} = 7.7\text{--}200$ GeV are shown in Fig. 9, and the results are compared with the standard $\text{FB}_{\text{relative}}$ method [Eq. (12)]. The shapes of $b(\Delta\eta)$ are flat, and the values of b are much higher than the results of Eq. (12). We consider that the FB correlation strengths b of this simple $\text{FB}_{\text{relative}}$ method [Eq. (C2)] are dominated by the mixing of events of different centralities for a certain reference multiplicity N_{ref} , and this phenomenon is caused by ignoring the fluctuation of N_{ref} . Anyhow, there are also nearly no differences between b of different centrality windows.

APPENDIX D: DERIVATION OF FB CORRELATION STRENGTH b OF THE MC SOURCE

In an event, c and u stand for numbers of correlated and uncorrelated particles, and c_f, c_b, u_f , and u_b stand for the numbers of correlated-forward, correlated-backward, uncorrelated-forward, and uncorrelated-backward particles, respectively. For the MC model in Sec. III,

$$\langle c_f \rangle = \sum_{c_f=0}^{c/2} c_f \binom{c}{c_f} (2p)^{c_f} (1-2p)^{\frac{c}{2}-c_f} = pc, \\ \langle c_f^2 \rangle = \sum_{c_f=0}^{c/2} c_f^2 \binom{c}{c_f} (2p)^{c_f} (1-2p)^{\frac{c}{2}-c_f} = p^2 c^2 + p(1-2p)c,$$

$$\begin{aligned}
 \langle u_f \rangle &= \sum_{u_f=0}^u u_f \binom{u}{u_f} p^{u_f} (1-p)^{u-u_f} = pu, \\
 \langle u_f^2 \rangle &= \sum_{u_f=0}^u u_f^2 \binom{u}{u_f} p^{u_f} (1-p)^{u-u_f} = p^2 u^2 + p(1-p)u, \\
 \langle u_f u_b \rangle &= \sum_{u_{bf}=0}^u \sum_{u_f=0}^{u_{bf}} u_f (u_{bf} - u_f) \binom{u_{bf}}{u_f} \left(\frac{1}{2}\right)^{u_{bf}} \\
 &\quad \times \binom{u}{u_{bf}} (2p)^{u_{bf}} (1-2p)^{u-u_{bf}} \\
 &= p^2 u^2 - p^2 u, \tag{D1}
 \end{aligned}$$

where $u_{bf} = u_b + u_f$, and $\langle c_b \rangle = \langle c_f \rangle$, $\langle u_b \rangle = \langle u_f \rangle$, $\langle c_b^2 \rangle = \langle c_f^2 \rangle = \langle c_f c_b \rangle$ (because of $c_f = c_b$) are used in the following derivation. The parameter p is equal to $\delta\eta/(\eta_{\max} - \eta_{\min})$ where $\delta\eta$ is the forward (or backward) bin width and $(\eta_{\max}, \eta_{\min})$ is

the range of η in the MC model. Therefore, the variables of Eq. (3) can be expressed as

$$\begin{aligned}
 \langle N_f \rangle &= \langle c_f + u_f \rangle = \langle c_f \rangle + \langle u_f \rangle, \\
 \langle N_b \rangle &= \langle c_b + u_b \rangle = \langle c_b \rangle + \langle u_b \rangle, \\
 \langle N_f^2 \rangle &= \langle (c_f + u_f)^2 \rangle = \langle c_f^2 \rangle + \langle u_f^2 \rangle + 2\langle c_f \rangle \langle u_f \rangle, \\
 \langle N_f N_b \rangle &= \langle (c_f + u_f)(c_b + u_b) \rangle \\
 &= \langle c_f c_b \rangle + \langle u_f u_b \rangle + \langle c_f \rangle \langle u_b \rangle + \langle u_f \rangle \langle c_b \rangle. \tag{D2}
 \end{aligned}$$

By taking Eq. (D1) into Eq. (D2), $D_{bf}^2 = \langle N_b N_f \rangle - \langle N_b \rangle \langle N_f \rangle$ and $D_{ff}^2 = \langle N_f^2 \rangle - \langle N_f \rangle^2$ can be expressed as

$$\begin{aligned}
 D_{bf}^2 &= p(1-2p)c - p^2 u, \\
 D_{ff}^2 &= p(1-2p)c + p(1-p)u. \tag{D3}
 \end{aligned}$$

By taking $c = \alpha N_{ch}$ and $u = (1-\alpha)N_{ch}$ into Eq. (D3), $b = D_{bf}^2/D_{ff}^2$ can be expressed as Eq. (13).

-
- [1] Y. V. Kovchegov, E. Levin, and L. McLerran, *Phys. Rev. C* **63**, 024903 (2001).
- [2] S. Uhlig, I. Derado, R. Meinke, and H. Preissner, *Nucl. Phys. B* **132**, 15 (1978).
- [3] K. Alpgard *et al.* (UA5 Collaboration), *Phys. Lett. B* **123**, 361 (1983).
- [4] G. J. Alner *et al.* (UA5 Collaboration), *Nucl. Phys. B* **291**, 445 (1987).
- [5] R. Ansorge *et al.* (UA5 Collaboration), *Z. Phys. C* **37**, 191 (1988).
- [6] J. Dias de Deus, J. Kwiecinski, and M. Pimenta, *Phys. Lett. B* **202**, 397 (1988).
- [7] T. Alexopoulos *et al.* (E735 Collaboration), *Phys. Lett. B* **353**, 155 (1995).
- [8] Y.-X. Ye, S.-S. Wang, X. Zhou, C.-G. Xiao, J. Zhang, and D.-P. Zhu, *Phys. Lett. B* **382**, 196 (1996).
- [9] P. Brogueira, J. Dias de Deus, and C. Pajares, *Phys. Lett. B* **675**, 308 (2009).
- [10] T. J. Tarnowsky (Star Collaboration), *Indian J. Phys.* **85**, 1091 (2011).
- [11] G. Aad *et al.* (ATLAS Collaboration), *J. High Energy Phys.* **07** (2012) 019.
- [12] J. Adam *et al.* (ALICE Collaboration), *J. High Energy Phys.* **05** (2015) 097.
- [13] B. K. Srivastava (Star Collaboration), *Int. J. Mod. Phys. E* **16**, 3371 (2007).
- [14] B. I. Abelev *et al.* (Star Collaboration), *Phys. Rev. Lett.* **103**, 172301 (2009).
- [15] J. T. Terence, *J. Phys. Conf. Ser.* **230**, 012025 (2010).
- [16] L. Na, S. Shusu, T. Aihong, and W. Yuanfang, *J. Phys. G: Nucl. Part. Phys.* **39**, 115105 (2012).
- [17] Y.-L. Yan, D.-M. Zhou, B.-G. Dong, X.-M. Li, H.-L. Ma, and B.-H. Sa, *Phys. Rev. C* **79**, 054902 (2009).
- [18] Y.-L. Yan, B.-G. Dong, D.-M. Zhou, X.-M. Li, and B.-H. Sa, *Phys. Lett. B* **660**, 478 (2008).
- [19] J. Fu, *Phys. Rev. C* **77**, 027902 (2008).
- [20] R. He, J. Qian, and L. Huo, *Phys. Rev. C* **93**, 044918 (2016).
- [21] Z.-W. Lin, C. M. Ko, B.-A. Li, B. Zhang, and S. Pal, *Phys. Rev. C* **72**, 064901 (2005).
- [22] N. Amelin, N. Armesto, C. Pajares, and D. Sousa, *Eur. Phys. J. C* **22**, 149 (2001).
- [23] N. Armesto, C. Pajares, and D. Sousa, *Phys. Lett. B* **527**, 92 (2002).
- [24] P. Brogueira and J. Dias de Deus, *Phys. Lett. B* **653**, 202 (2007).
- [25] Y.-L. Yan, B.-G. Dong, D.-M. Zhou, X.-M. Li, H.-L. Ma, and B.-H. Sa, *Nucl. Phys. A* **834**, 320c (2010).
- [26] Y.-L. Yan, D.-M. Zhou, B.-G. Dong, X.-M. Li, H.-L. Ma, and B.-H. Sa, *Phys. Rev. C* **81**, 044914 (2010).
- [27] S. Ahmad, A. Chandra, M. Zafar, M. Irfan, and A. Ahmad, *Int. J. Mod. Phys. E* **22**, 1350066 (2013).
- [28] S. Ahmad, A. Khatun, S. Khan, A. Ahmad, and M. Irfan, *Adv. High Energy Phys.* **2015**, 8 (2015).
- [29] I. G. Altsybeev, G. A. Feofilov, and E. L. Gillies, *J. Phys. Conf. Ser.* **668**, 012034 (2016).
- [30] K. Vladimir and V. Vladimir, *J. Phys. Conf. Ser.* **668**, 012065 (2016).
- [31] V. Kovalenko and V. Vechernin, [arXiv:1502.01758](https://arxiv.org/abs/1502.01758).
- [32] V. Vechernin, *Nucl. Phys. A* **939**, 21 (2015).
- [33] N. Armesto, L. McLerran, and C. Pajares, *Nucl. Phys. A* **781**, 201 (2007).
- [34] M. Braun and C. Pajares, *Eur. Phys. J. C* **16**, 349 (2000).
- [35] L. McLerran and R. Venugopalan, *Phys. Rev. D* **49**, 2233 (1994).
- [36] E. Iancu, A. Leonidov, and L. McLerran, *Nucl. Phys. A* **692**, 583 (2001).
- [37] A. Capella and A. Krzywicki, *Phys. Rev. D* **18**, 4120 (1978).
- [38] A. Capella, U. Sukhatme, C. I. Tan, and J. Tran Thanh Van, *Phys. Rep.* **236**, 225 (1994).
- [39] W. D. Walker, *Phys. Rev. D* **69**, 034007 (2004).
- [40] B. K. Srivastava, R. P. Scharenberg, and T. J. Tarnowsky (Star Collaboration), *Int. J. Mod. Phys. E* **16**, 2210 (2007).
- [41] B. K. Srivastava (Star Collaboration), *J. Phys. G: Nucl. Part. Phys.* **35**, 104140 (2008).
- [42] A. Capella and J. Tran Thanh Van, *Phys. Rev. D* **29**, 2512 (1984).
- [43] C. Pajares, *Nucl. Phys. A* **854**, 125 (2011).
- [44] M. Skoby (Star Collaboration), *Nucl. Phys. A* **854**, 113 (2011).
- [45] X.-N. Wang and M. Gyulassy, *Phys. Rev. D* **44**, 3501 (1991).

- [46] S. De, T. Tarnowsky, T. K. Nayak, R. P. Scharenberg, and B. K. Srivastava, *Phys. Rev. C* **88**, 044903 (2013).
- [47] T. Lappi and L. McLerran, *Nucl. Phys. A* **832**, 330 (2010).
- [48] A. Olszewski and W. Broniowski, *Phys. Rev. C* **88**, 044913 (2013).
- [49] J. Jia, S. Radhakrishnan, and M. Zhou, *Phys. Rev. C* **93**, 044905 (2016).
- [50] V. Khachatryan *et al.* (CMS Collaboration), *J. High Energy Phys.* **09** (2010) 091.
- [51] B. I. Abelev *et al.* (STAR Collaboration), *Phys. Rev. C* **80**, 064912 (2009).
- [52] C. Pruneau, S. Gavin, and S. Voloshin, *Phys. Rev. C* **66**, 044904 (2002).
- [53] V. Vechernin, [arXiv:1305.0857](https://arxiv.org/abs/1305.0857).
- [54] A. Monnai and B. Schenke, *Phys. Lett. B* **752**, 317 (2016).
- [55] A. Bzdak and D. Teaney, *Phys. Rev. C* **87**, 024906 (2013).